Monte Carlo track structure simulations and the biophysical model NanOx in targeted radionuclide therapy

CELLDOSE collaboration: M E Alcocer-Ávila[1], A Larouze[1], E Hindié[2,3] and C Champion[1]
PICTURE collaboration: M E Alcocer-Ávila[4], V Levrague[5], R Delorme[5], E Testa[4] and M Beuve[4]

[1]CELIA, Université de Bordeaux, 33405 Talence, France
[2]INCIA, Université de Bordeaux, CHU de Bordeaux - Service de Médecine Nucléaire, 33604 Pessac, France
[3]Institut Universitaire de France, 75231 Paris Cedex 05, France
[4]IP2I, Université Claude Bernard Lyon 1, 69622 Villeurbanne Cedex, France
[5]LPSC, Université Grenoble Alpes, 38026 Grenoble Cedex, France

March 15, 2022

TRT with Auger electron and α-particle emitters

- TRT using Auger electrons (AEs) and α-particles has generated much interest in the last decades
- AEs and α-particles are high linear energy transfer (LET) radiations able to deliver cytotoxic radiation doses to tumors while sparing the healthy tissue, in contrast to β^--particles and X-rays
- Computer simulations may be used for pre-clinical dosimetry of promising AE and α-particle emitters

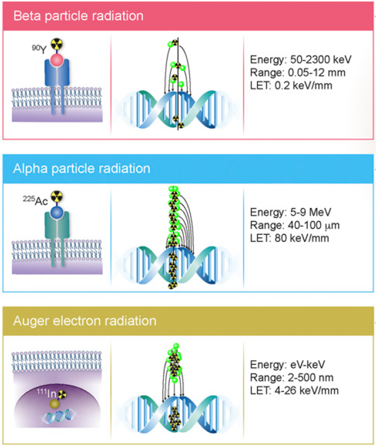

Figure 1: Comparison of radioactive particles for TRT [1]

The role of Monte Carlo track structure (MCTS) simulations in TRT

- MC codes have a long history in radiation physics and radiation biology ("gold standard")
- Track structure simulations follow radiations on an event-by-event basis
- Very time-consuming, but ideal for subcellular volumes, low-energy radiations and DNA damage studies
- Features make MCTS simulations interesting for accurate radiation dosimetry in TRT

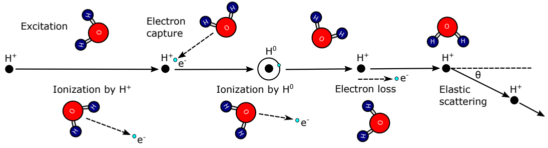

Figure 2: Illustration of the event-by-event approach for protons in water

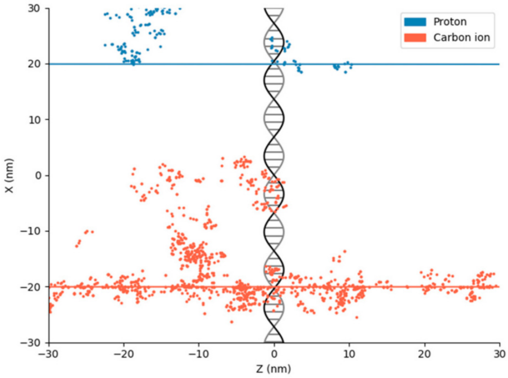

Figure 3: Illustration of the track structure of a 10 MeV proton and 200 MeV carbon ions [2]

Cellular dosimetry with CELLDOSE

CELLDOSE [3] simulations for evaluating radionuclides for TRT:

- **β^--emitters**: ^{90}Y, ^{131}I, ^{177}Lu, ^{161}Tb
- **AE-emitters**: ^{71}Ge, ^{103m}Rh, ^{119}Sb, ^{125}I, ^{161}Ho, ^{189m}Os, ^{193m}Pt, ^{195m}Pt
- **α-emitters**: ^{211}At, ^{212}Pb/^{212}Bi, ^{213}Bi, ^{223}Ra, ^{225}Ac and ^{227}Th
- Calculation of S-values (Gy·Bq^{-1}·s^{-1}) and normalized absorbed doses assuming **cell nucleus** as critical target

- Case of a **single cell** and a **small cell cluster**

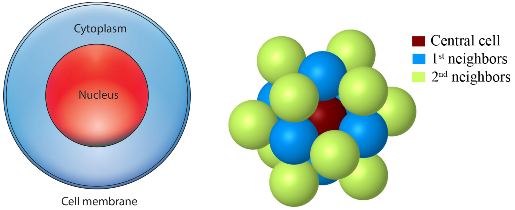

Figure 4: Left: single cell with spherical geometry ($R_C = 7\ \mu$m, $R_N = 5\ \mu$m); right: cell cluster (19 cells)

- **Different radionuclide distributions**: cell surface, intracytoplasmic, intranuclear and whole cell

Cellular dosimetry with CELLDOSE

Single cell

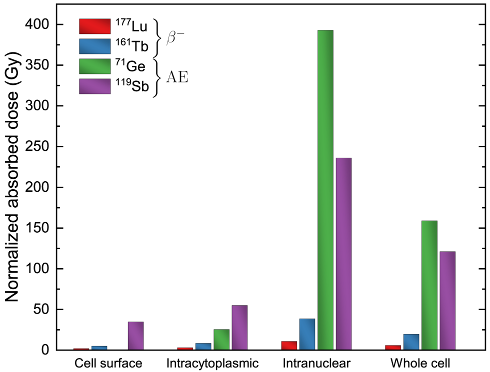

Figure 5: Normalized absorbed doses to the **nucleus of a single cell** for different distributions of selected β^--particle and AE emitters

Cell cluster

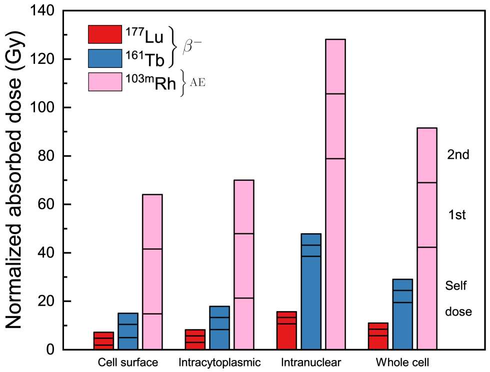

Figure 6: Normalized absorbed doses to the **nucleus of the central cell in a cluster** for different distributions of selected β^--particle and AE emitters

Towards more comprehensive approaches

Some limitations in the previous studies include:

- Energy deposition events described exclusively during the physical stage.
  → Need of accounting for processes occuring in later stages of radiation action (Fig. 7)
- Need of modeling realistic cell geometries and complex multicellular systems

Other simulation tools and biophysical models may be applied for reaching more clinically relevant endpoints, e.g. the **biological dose** for ion irradiations

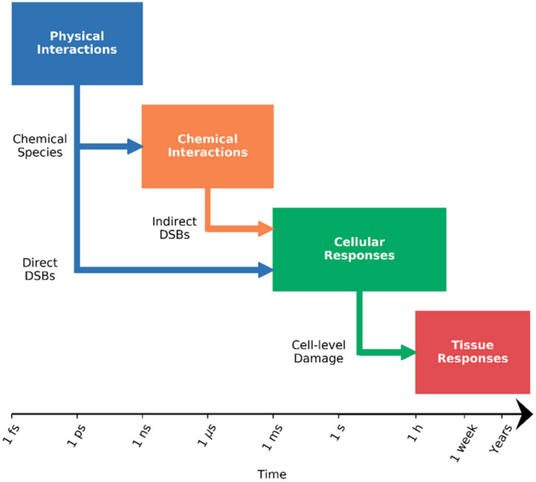

Figure 7: Stages of radiation action [2]

Planning Innovative Cancer Therapies Using RadioElements

The **PICTURE project** focus on the optimization of dosimetry calculations for targeted alpha therapy (TAT) and boron neutron capture therapy (BNCT), considering:

- **Biological dose** modeling: **NanOx** + Geant4-DNA
- The impact of different **radionuclide distributions** in cells, including heterogeneities
- The role of **nuclear** and **extra-nuclear** sensitive sites in radiation-induced cell death

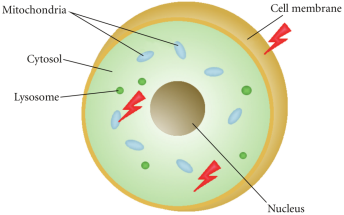

Figure 8: Potentially important extra-nuclear sites in a cell [6]

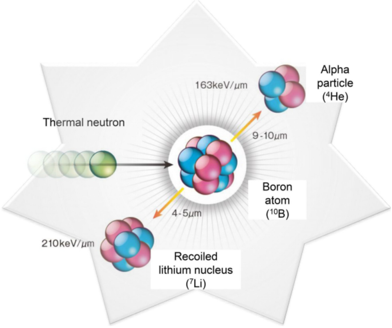

Figure 9: Principle of boron neutron capture therapy (BNCT) [7]

The PICTURE project

- Creation of a database of **realistic 3D cell geometries** based on confocal microscopy
- Experimental studies with different cell lines (CHO-K1, SQ20B and U87) irradiated in conditions of full (FCT) and partial cell transversal (PCT)

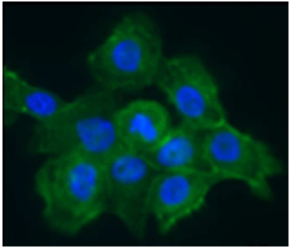

Figure 10: Micrograph of SQ20B cells [8]

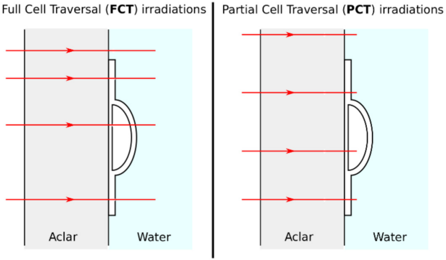

Figure 11: Cell irradiation conditions with broad ion beams

The NanOx biophysical model

- Prediction of cell survival for ion irradiations
- Considers stochastic nature of radiation at different scales. Two types of biological events: **local lethal events (LLE)** and **global events (GE)**:

LLE → inactivation of **nanometric targets**
GE → accumulation of sublethal lesions including physico-chemical processes (**micrometric scale**)

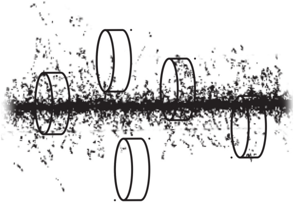

Figure 13: Irradiation of cells by a given radiation impact [9]

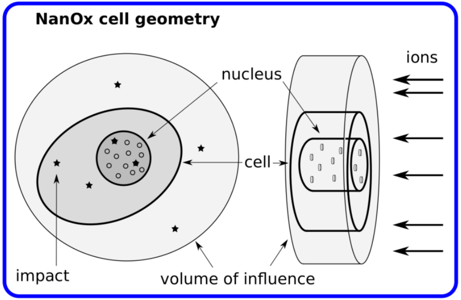

Figure 12: Current cell geometry in NanOx simulations

$$S = S_{LLE} \times S_{GE} \quad (1)$$

The NanOx biophysical model

- 5 parameters derived from experimental data:

  → **Sensitive volume radius**

  → 3 parameters characterizing the **effective local lethal function**, used for calculating the survival to LLE (Fig. 14)

$$F(z) = \frac{h}{2}\left[1 + \mathrm{erf}\left(\frac{z - z_0}{\sigma}\right)\right] \qquad (2)$$

  → **Quadratic coefficient** β_r for reference (photon) irradiation

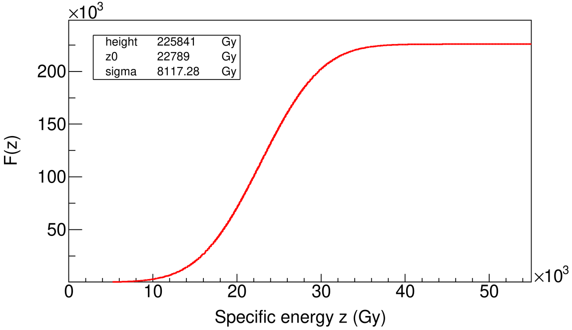

Figure 14: Effective local lethal function for the V79 cell line

The NanOx biophysical model

- NanOx has been applied to study the radiation response of several cell lines in the context of hadrontherapy [10]
- α and β coefficients can be obtained from a LQ fit to NanOx results (Fig. 16)

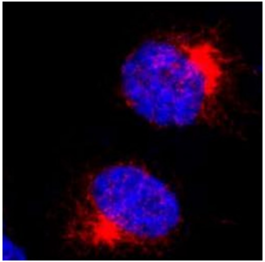

Figure 15: Image of HSG cells [11]

- **NanOx predictions are more accurate than the ones of other biophysical models**

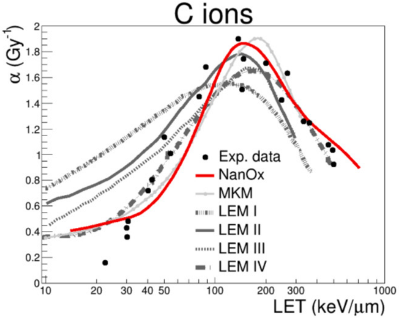

Figure 16: α values of HSG cells for carbon ions. The graph shows experimental data as well as the predictions of several biophysical models, including NanOx [12]

Conclusions

- MCTS codes remain the best computational tools for investigating ionizing radiation interactions at the subcellular level, including preclinical studies for TRT
- Current challenges for realistic simulations of TRT treatments include the consideration of complex cell geometries, heterogeneous distributions of radiation sources in the cells and extra-nuclear sensitive sites
- The ongoing PICTURE project is expected to improve the biological dose estimation for innovative radiation therapies, especially TAT and BNCT
- **Need of experimental data regarding the 4D biodistribution of radionuclides with subcellular resolution**

Thank you for your attention

Merci pour votre attention

References

[1] S. Poty, L. C. Francesconi, M. R. McDevitt, et al., *J. Nucl. Med.* **2018**, *59*, 878–884.

[2] S. J. McMahon, K. M. Prise, *Cancers* **2019**, *11*, 205.

[3] C. Champion, P. Zanotti-Fregonara, E. Hindié, *J. Nucl. Med.* **2008**, *49*, 151–157.

[4] B. Vaziri, H. Wu, A. P. Dhawan, et al., *J. Nucl. Med.* **2014**, *55*, 1557–1564.

[5] T. Sato, Y. Iwamoto, S. Hashimoto, et al., *J. Nucl. Sci. Technol.* **2018**, *55*, 684–690.

[6] Z. Kuncic, H. L. Byrne, A. L. McNamara, et al., *Comput. Math. Method. M.* **2012**, *2012*, 1–9.

[7] M. Suzuki, *Int. J. Clin. Oncol.* **2020**, *25*, 43–50.

[8] J.-B. Guy, B. Méry, E. Ollier, et al., *Sci. Rep.* **2017**, *7*, 12207.

[9] M. Cunha, C. Monini, E. Testa, et al., *Phys. Med. Biol.* **2017**, *62*, 1248–1268.

[10] C. Monini, É. Testa, M. Beuve, *Acta Phys. Pol. B* **2017**, *48*, 1653.

[11] Y.-J. Kim, Y. Jo, Y.-H. Lee, et al., *Sci. Rep.* **2019**, *9*, 17648.

[12] C. Monini, G. Alphonse, C. Rodriguez-Lafrasse, et al., *Phys. Imaging. Radiat. Oncol.* **2019**, *12*, 17–21.

Appendix: Physical properties of some β^--emitters

Radionuclide	^{131}I	^{90}Y	^{177}Lu	^{161}Tb
Half-life (day)	8.02	2.67	6.647	6.906
β^--particles mean energy (keV)	182	932.9	133.3	154.3
Daughter nucleus	^{131}Xe (stable)	^{90}Zr (stable)	^{177}Hf (stable)	^{161}Dy (stable)
CE (intensity per decay)	6.46%	0.01%	15.47%	142%
CE (energy per decay in keV)	9.57	0.2	13.52	39.28
CE energy range in keV†	45.6 – 602.4	1742.7	6.2 – 206.3	3.3 – 98.3
AE (intensity per decay)	69.75%	0.13%	111.65%	1096.4%
AE (energy per decay in keV)	0.41	0.0007	1.13	8.94
AE energy range in keV	0.026 – 32.9	0.022 – 1.8	0.01 – 61.7	0.018 – 50.9
Total electron energy per decay (keV)	191.8	933.1	147.9	202.5
γ or X-ray radiation useful for imaging (energy in keV and % abundance)*	364.5 (81.7%) 330 (1.6%) 284.3 (6.1%) 80.2 (2.6%)	–	208 (11%) 113 (6.4%)	75 (10.2%)
Photons (energy per decay in keV)	382.7	–	35.1	36.35
Total energy per decay in keV (photons + electrons)	574.5	933.1	183	238.9
% of energy emitted as electrons	33.4%	∼100%	80.8%	84.8%
% of energy emitted as photons	66.6%	∼0%	19.2%	15.2%

Appendix: Physical properties of some AE-emitters

Radionuclide	^{71}Ge	^{103m}Rh	^{119}Sb	^{125}I
Half-life (day)	11.43	0.039	1.591	59.4
Type of decay (%)	EC (100%)	IT (100%)	EC (100%)	EC (100%)
Daughter nucleus	^{71}Ga (stable)	^{103}Rh (stable)	^{119}Sn (stable)	^{125}Te (stable)
CE (intensity per decay)	–	99.06%	83.97%	94.47%
CE (energy per decay in keV)	–	34.97	16.97	7.28
CE energy range in keV†	–	16.56 – 39.76	19.4 – 23.9	3.7 – 35.5
AE (intensity per decay)	520.5%	587.94%	2368%	2300%
AE (energy per decay in keV)	5.01	2.72	8.86	11.96
AE energy range in keV	0.012 – 10.1	0.034 – 22.28	0.011 – 27.9	0.023 – 30.3
Total electron energy per decay (keV)	5.01	37.69	25.83	19.24
γ or X-ray radiation useful for imaging (energy in keV and % abundance)*	–	–	–	–
Photons (energy per decay in keV)	4.07	1.65	23.14	42.5
Total energy per decay in keV (photons + electrons)	9.08	39.34	48.97	61.74
% of energy emitted as electrons	55.2%	95.8%	52.8%	31.2%
% of energy emitted as photons	44.8%	4.2%	47.2%	68.8%
photon-to-electron energy ratio (p/e)	0.81	0.04	0.90	2.21